

Analysis of the Performances in Retrieved Atmospheric Profiles with Radio-Occultation Methods by Considering Different Sources of Error and Different Processing Techniques

Carmelo Carrascosa-Sanz⁽¹⁾, Laura Fernández-Pérez⁽¹⁾, Juan-Manuel Salcedo⁽¹⁾, David Modrego-Contreras⁽¹⁾,
Marc Loiselet⁽²⁾, Jacob Christensen⁽³⁾, Mikael Hägg⁽³⁾

⁽¹⁾ GMV S.A.

Isaac Newton 11, P.T.M. Tres Cantos. E-28760 Madrid, Spain

Email: ccarrascosa@gmv.es; lfernandez@gmv.es; jmsalcedo@gmv.es; dmodrego@gmv.es

⁽²⁾ ESTEC/ESA

Keplerlaan 1 - P.O Box 299-2200 AG Noordwijk ZH, The Netherlands

Email: Marc.Loiselet@esa.int

⁽³⁾ Saab Ericsson Space

Saab Ericsson Space AB, SE-405 15 Göteborg, Sweden

Email: jacob.christensen@space.se; mikael.hagg@space.se

INTRODUCTION

Radio-Occultation method is more and more used to retrieve atmospheric conditions using limb sounding geometry. This technique requires very accurate measurements in order to minimise the numerous sources of error that are involved in the data processing. In the frame of an ESTEC/ESA contract, GMV has developed a simulation tool where all error sources can be adjustable as desired. This is part of the METOP-GRAS Ground Processor Prototype (GPP, [1]), and it is part of the GRAS contract, led by SES. The GPP is a software tool intended to isolating the atmospheric contribution in GPS Radio-Occultation sounding measurements. The purpose of the GPP is the development and validation of the algorithms to convert the GPS observables into atmospheric properties, and to verify the end-to-end performances of the technique.

In the frame of the GPP validation, a simulation/verification environment has been developed. This environment is named GPP Test Software. This software tool simulates all the input data needed for the processing of radio occultation measurements as they were generated in real life. GPS measurements are generated with a great level of representativeness as they were tracked by a receiver, considering all the components; range, clocks, relativistic effects, receiver thermal noise, local multipath, hardware delays, cycle slips, atmospheric and ionospheric components. In particular, atmospheric/ionospheric components are simulated with a three-dimensional (3D) ray tracer and diffraction conditions can be also included through a Wave Optic Propagator (WOP, [2]) module. Apart to the GPS measurements tracked by the receiver, the GPP Test SW provides:

- Highly accurate GPS measurements tracked by all the ground stations in the system. These data will be useful when differential schemes are selected in the processing.
- Information of the recovered orbits of the emitters and receiver as they were computed by the ground system (Precise Orbit Determination).
- Information of the recovered clock errors for all clocks in the system as they were computed by the ground system (Clock Estimation).
- Attitude Error information as they were provided by spacecraft sensors.

The errors in these additional estimation modules, position, clocks and attitude, are properly characterised. Moreover, the GPP Test SW provides as output all the components and errors used in the simulation. These data is used as truth to evaluate the end-to-end performances in the radio occultation processes.

In the GPP Test SW, all sources of errors and error components can be activated/deactivated separately and the user can configure them. This allows the performance assessment of each individual error contribution and the propagation of this error to the retrieved atmospheric profile. Finally, as the GPP implements different algorithms for the compensation of clock errors and for the inversion to atmospheric profiles (geometrical optics, [3] and back-propagation, [4]), the performances of the different algorithms can be evaluated.

This paper provides the main results assessed with the processing of simulated data through the GPP by considering the different clock correction schemes; differential schemes, methods based on external clock information and methods based on calibration with an external atmospheric model. The effects of the different sources of error provide a complete error budget on retrieved atmospheric measurements. In particular, the capabilities for retrieval of atmospheric diffraction effects are addressed.

DESCRIPTION OF THE EVALUATED PROCESSING TECHNIQUES

The main GPS measurement is the carrier phase because of its high accuracy. The carrier phase components can be expressed as follows:

$$\mathbf{f} = \mathbf{I} \cdot N + \mathbf{r} + c \cdot (T_{Ins} - T_{SV}) + E_{Ins} - d_{ion} + d_{tro} + mp + \mathbf{e}_f \quad (1)$$

Where; \mathbf{f} is the complete carrier phase measurement. \mathbf{r} is the geometric distance between the center of phases of the emitting (at GPS satellite) and receiving (at LEO) antennas. T_{Ins}, T_{SV} are the clock offsets at receiver and emitter which can include relativistic effects. E_{Ins} is the hardware delay in the instrument. d_{ion} is the ionospheric delay and d_{tro} is the tropospheric delay. \mathbf{I} is the wavelength and N is the integer ambiguity parameter, which takes into account possible cycle slips. \mathbf{e}_f is the receiver thermal noise in carrier phase and mp is the multipath delay on carrier phase.

In radio occultation techniques, all the components present in the carrier phase measurement must be cancelled excepting the term due to the atmosphere. Hence, the useful terms for atmospheric sounding purposes are ionospheric and tropospheric delays. The GPP considers sequentially the following corrections for the carrier phase:

- Correction for instrument hardware delays. The E_{Ins} is compensated for by means of a calibrated instrument database. Effect of different hardware components is cancelled separately; antenna and electronic unit effects.
- Correction for geometrical range. The \mathbf{r} term is cancelled by using as reference:
 - The position/velocities of the spacecraft provided by ground segment, i.e Precise Orbit Determination (POD).
 - Attitude information.
- Relativistic effects. These terms are present in geometrical range and in the clock errors.
- Clock correction. The clock effects due to the emitter and receiver are compensated through different techniques:
 - Differential techniques, using auxiliary links to compensate for clocks by differentiation. Fig. 1 shows the five possible differential techniques considered in the GPP; ND, SD1, SD2, DD and DD2.
 - Frequency Bias Estimation (FBE). This method estimates the clock by comparing with an atmospheric model.
 - POD Based Clock Correction (PBCC). POD produces as output an estimate of all the clocks in the process.

Note that combination of different techniques is possible.

- Cycle slip detection and correction. Variation in the unknown integer ambiguity, $\mathbf{I} \cdot N$, must be detected and corrected. Note that the integer ambiguity term must not be solved because the atmospheric profiles are functions of the atmospheric Doppler effect.
- Filtering of thermal noise. Different filters have been designed and implemented in the GPP to avoid the propagation of thermal noise in the occultation flow.

Once the atmospheric components in the GPS measurements have been isolated, i.e. d_{ion} and d_{tro} , the atmospheric properties can be derived at different levels (Fig.2):

- Bending angle as a function of impact parameters. The GPP produces these level1b products. Two different inversion methods have been implemented in the GPP; a method based in Geometrical Optics (GO) theory and a method based in Back-Propagation (BP) concept in order to solve atmospheric diffraction conditions.
- Refractivity profiles. This is a level 2 product. The Abel Transform converts from bending angle to refractivity profiles. This algorithm has not been considered in the GPP.

The analysis described in this paper assesses the performances at the bending angle level.

Note that all the inaccuracies associated to the correction process will be propagated to the residual carrier phase.

Examples of these inaccuracies are:

- Calibration errors in the instrument database, when performing the instrument correction for receiver.
- Inaccuracies in range POD products. The errors in the spacecraft position and velocity will be propagated into the sounding chain due to the range correction and the inversion algorithms.
- When using differential schemes, the error components in the auxiliary links must be mitigated; geometrical range, atmospheric delays, local multipath, thermal noise and cycle slips.
- When using FBE, inaccuracies in the reference model will be propagated to bending angle level.
- When using PBCC, the errors in the estimated clocks by POD will be propagated into the sounding data.
- Obviously, any error in the detection/correction of cycle slip will be propagated to bending angle, when using geometrical optic retrieval.

As atmospheric properties depend on Doppler effect, those constant-like effects in carrier phase will not be propagated to bending angle.

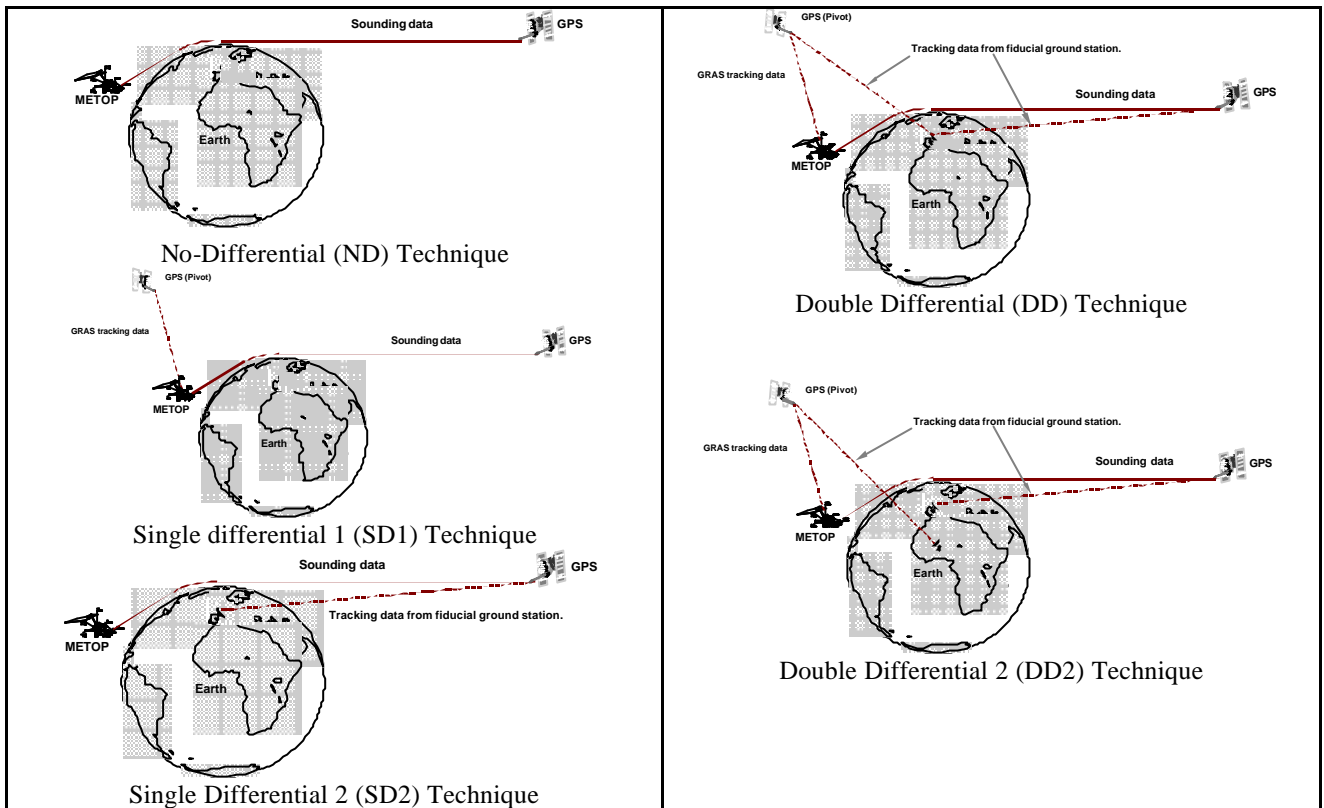


Fig. 1. Possible Differential Techniques for Clock Correction

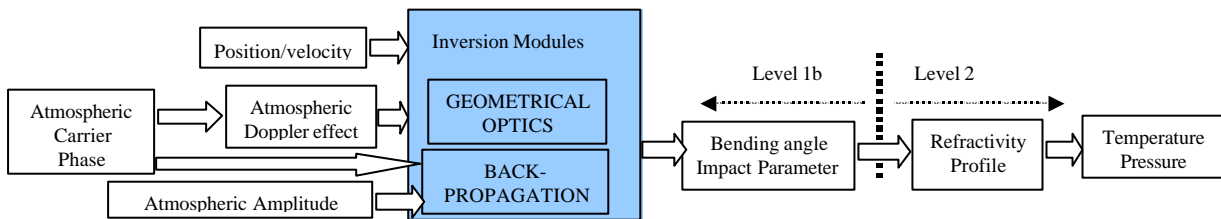


Fig. 2. Overview of Processing from Residual Atmospheric Carrier Phase

DESCRIPTION OF THE INPUT DATA FOR THE SIMULATIONS

Considered Occultation Geometry

Two METOP occultation geometries are analyzed, representing a slow velocity occultation and a normal velocity occultation. To represent the occultation geometry, two parameters are selected; the tangent point inversion rate at 30 km. altitude, $dh/dt|_{30Km}$, and the elapsed time between 70 km. and 30 km, $\Delta T_{70-30Km}$. The geometry parameters of these occultations are depicted in Table 1.

Table 1. Considered occultation geometries for the analysis

	Slow	Normal
$dh/dt _{30Km}$ (Km/Sec)	1.5810	2.6173
$\Delta T_{70-30Km}$ (Sec)	23.5912	14.2446

Reference Atmospheric Profile

A bi-exponential analytic neutral atmosphere is used for sounding link. Equation (2) shows this analytical function and Table 2 describes the meaning of the parameter and the value considered for the simulation. Two atmospheric models

have been considered; one model represents a thin-dry atmosphere (representative of a dry polar environment) and the other is for a dense-wet atmosphere (representative of tropical environment). The ray tracer will be used as forward modeling method because there is no diffraction effects.

$$N(h) = N_{0d} \cdot e^{-(h/H_d)} + N_{ow} \cdot e^{-(h/H_w)} \quad (2)$$

Table 2. Analytical neutral atmospheric model.

Parameter	Thin-dry	Dense-Wet
N_{0d} Dry refractivity at surface	200 N-units.	300 N-units
H_d Dry scale height	7.5 Km.	7.9 km
N_{ow} Wet refractivity at surface	0 N-units.	100 N-units
H_w Wet scale height	2.5 Km.	2.5 km

Atmospheric diffraction effects can be considered by adding to (2), a perturbation effect considering a bump (3):

$$N(h) = N_{0d} \cdot e^{-(h/H_d)} + N_{ow} \cdot e^{-(h/H_w)} + BA \cdot e^{-(h-BH)^2 / BW} \quad (3)$$

where; BA is the size of the bump (in N-units), BH is the height position of the bump (in km) and BW is the scale factor of the bump related with the aperture (in km²). In this simulation campaign, the values have been set to BA = 4 N-units, BH = 6 km and BW = 0.009 km². This perturbation represents a medium multipath effect $\partial N / \partial h|_{\max} = 57$ N - units/km , and a perturbation width of about 150 m. The purpose is that back-propagation method is able to retrieve this perturbation.

Ionospheric Model

The ionosphere is described by electron density, N_x . N_x is a double Chapman profile with height, “h”, and determined by the parameters N_E , Z_E , H_E , N_F , Z_F , and H_F as:

$$N_x = N_E \cdot e^{\frac{1}{2}(1-Z_E-e^{-Z_E})} + N_F \cdot e^{\frac{1}{2}(1-Z_F-e^{-Z_F})} \quad (4)$$

where $Z_E = \frac{h-Z_E}{H_E}$ and $Z_F = \frac{h-Z_F}{H_F}$. The model parameter values are:

Table 3. Considered parameters in the ionospheric model

N_E	$2e^{11}$ [el/m3]
H_E	10 [km]
Z_E	105 [km]
N_F	$3e^{11}$ [el/m3]
H_F	50 [km]
Z_F	300 [km]

Simulated Error Component

The GPP Test Software can select the error introduced in the data simulation. This allows simulating different cases corresponding to the isolated effect of each individual source of error. In both GPP and GPP Test SW, errors can be turned off by setting the error magnitude of the error modeling to zero, i.e. no clock error, no thermal noise, no ionosphere etc. In addition, simulations where all errors are turned on simultaneously can be considered. A summary of the considered errors is provided in following tables. Table 4 describes the simulated receiver errors. Table 5 considers the errors due to the ground segment network. Table 6 includes the error characteristics of the GPS clocks. In addition to these error components, relativistic effects are also considered. According to [5], relativistic effects affect the emitting GPS satellite, the receiving LEO satellite and the fiducial ground stations. All these observers are in movement and they do not have the same gravitational potential.

Table 4. Considered Receiver Errors in the Simulation

Error Component	Value/Characterization	Comment
Receiver thermal noise	GRAS Instrument model with AS ON	GRAS manufacturer (SES), [6], has developed an instrument model that characterizes the receiver thermal noise according to GRAS instrument. This instrument model is fully integrated in the GPP Test Software. In the level0 to level 1b process, the different filters in the occultation flow must mitigate this effect.
Receiver Cycle Slips	GRAS Instrument Model	GRAS Instrument model is able to simulate cycle slips. In the level0 to level 1b process, there is a specific algorithm to detect and correct for cycle slips.
Receiver Hardware Delays	GRAS Instrument Database	GRAS manufacturer (SES) has calibrated GRAS on-ground. The GPP Test SW includes this instrument database to simulate the errors. In the level0 to level1b process, the instrument correction algorithm is devoted to mitigate this effect. As the same instrument database is considered in the compensation, this effect is completely cancelled.
Receiver Clock Error	$D_{Clock} = 1 \cdot 10^{-7} [s/s]$ $A_{Clock} = 5 \cdot 10^{-14} [s/s^2]$ $ADEV_{Clock} = 1 \cdot 10^{-12} [s/s]$	The clock error is simulated as: $\Delta T_R(T) = D_{Clock} \cdot T + A_{Clock} \cdot T^2 + f(ADEV_{Clock})$. D_{Clock} is the clock-drift term. A_{Clock} is the clock-acceleration term (i.e. the frequency drift). $f(ADEV_{Clock})$ Represents the short-term stability of the clock given by the Allan Deviation.
Receiver Local Multipath	According to GRAS Specs. [7].	In sounding data: $v_{error} \approx 50 \text{ mm/s}$ and $a_{error} \approx 1.5 \text{ mm/s}^2$ In zenith data: $v_{error} \approx 40 \text{ mm/s}$ and $a_{error} \approx 2 \text{ mm/s}^2$ In the level0 to level1b process, there is not implemented any specific algorithm for multipath mitigation.

Table 5. Considered Ground Segment Network Errors in the Simulation

Error Component	Value/Characterization	Comment
Metop attitude	According to GRAS Specs. [7].	Pointing Knowledge (RMS value) = 0.017 deg. Absolute Rate Error (RMS value) = 0.005 deg/s. Frequency of the Error = [0 4] Hz. This error is introduced in the process in the geometrical range correction.
POD range errors: GPS & METOP	Bias error + errors in the orbit harmonics	Bias in position: 1 meter error Orbit harmonics: 0.1 mm/s in the 1st and 2nd orbit harmonics This error is introduced in the process in the geometrical range correction.
POD range errors: GPS & METOP & Ground Stations	Orbit harmonics + a gaussian noise.	For METOP receiver: 300 ps in 1'st METOP Orbit Harmonic, 80 ps in 2'nd METOP Orbit Harmonic, and Sample to Sample error Variation = 100 ps. For GPS clock and GS clocks: 130 ps in 1'st METOP Orbit Harmonic, 50 ps in 2'nd METOP Orbit Harmonic, and Sample to Sample error Variation = 100 ps. This error is introduced in the process in the clock correction if PBCC is activated.
FBE modeling error	0.2 μrad bias in bending angle.	The FBE modeling error can not be controlled by the simulator tool because it is due to the difference between atmospheric model and real atmosphere. A FBE modeling error of 0.2 μrad is added the simulation results when FBE is applied.

Table 6. Considered Emitter Clock Errors in the Simulation

Error Component	Value/Characterization	Comment
GPS clock error without SA	Drift error + acceleration error + short term instability	The clock is simulated as the receiver clock error model above and according to GRAS Specs. [7]. $D_{Clock} = 1 \cdot 10^{-10} [s/s]$, $A_{Clock} = 5 \cdot 10^{-15} [s/s^2]$, $ADEV_{Clock} = 2 \cdot 10^{-12} [s/s]$
SA without GPS clock error	Range = 30 m Velocity = 0.2 m/s Acceleration = 4 mm/s	The Rater model [8] has been considered

Table 7. Considered errors in the auxiliary data

Error Component	Value/Characterization	Comment
Fiducial clock error	Drift error + acceleration error + short term instability	The clock is simulated as the receiver clock above and according to GRAS-GPP specification [7]. $D_{Clock} = 1 \cdot 10^{-7} [s/s]$, $A_{Clock} = 1 \cdot 10^{-14} [s/s^2]$, $ADEV_{Clock} = 1 \cdot 10^{-13} [s/s]$
Fiducial thermal noise	As a function of the elevation (C/No). AS on	According to GRAS specification [1]. As an example: -at 30 deg $S_f = 0.227$ mm (L1 CA), $S_f = 7.801$ mm (L2 Y). -at 60 deg $S_f = 0.100$ mm (L1 CA), $S_f = 0.690$ mm (L2 Y).
Fiducial multipath	10 mm in 0.5 MHz on L1 and L2	According to GRAS Specs. [1]. In the level0 to level1b process, there is not any specific algorithm for multipath mitigation.
Fiducial tropospheric	Niell's model [9]	In the level0 to level1b process, there is a tropospheric correction for the ground station link.
Fiducial Ionospheric	Considering $1/f^2$, $1/f^3$ and $1/f^4$ [10]	In the level0 to level1b process, the ionospheric correction in the ground links is based on quadratic effects. Therefore, high order terms are not cancelled.

Configuration of Ground Processor Prototype

In the GPP all the corrections are activated: instrument correction, relativistic correction, range correction, clock correction, cycle slip correction. Among all the possible clock correction schemes, only the most relevant have been considered in this comparison; SD2+FBE, ND+PBCC, DD, and DD2+FBE.

The two retrieval schemes, GO and BP are activated. The filters are activated in order to mitigate the thermal noise; occultation filter, ionospheric filter in the neutral bending angle estimation, filter in the auxiliary data; and PBCC.

ANALYSIS OF RESULTS

Fig. 3 shows the error in neutral bending angle with the SD2-FBE configuration and considering a dense-wet atmosphere. Plot in the left corresponds to the normal velocity occultation, whereas plot in the right corresponds to the slow velocity occultation. The upper part of the profile corresponds to GO retrieval, and the lower part, below 19-km, corresponds to BP retrieval. The two profiles are combined by the GPP into a single output. In this figure, the threshold limits provided by the criteria of the maximum of 1 mrad or the 0.4% of the neutral bending angle are also depicted. This threshold limit is very interesting because it guarantees errors lower than $1 \text{ }^\circ\text{K}$ in the obtained temperature profiles at level 2 processing. Ten runs have been included in order to assess statistical results. The results for other methods are very similar, under the described error conditions in section above. Table 8 shows the percentage of the profile that is inside the above-defined limits, for different processing modes and for the two occultation geometries. The performances are very high for all the clock correction schemes, however:

- In the cases with FBE, an additional error of 0.2 mrad must be considered.
- In the cases with PBCC, degradation in the POD performances will reduce the performances.
- In the double-differences schemes, degradation in the performances of the receiver in the ground station receivers will degrade the performances.

Table 9 provides the bending angle error at 30 km for the different error contribution. The SD2, DD and DD2+FBE are considered with a thin-dry atmosphere and a slow occultation (worst case):

- A total error of about 0.5 $mrad$ is achieved at 30 km for all the processing schemes. This corresponds to a sub-Kelvin temperature error.
- It seems that the results is that DD performances are very similar than DD2+FBE results and generally better than the SD2 + FBE ones (about 0.15 $mrad$ worse). Of course, under the assumptions of the simulated data:
 - If the errors associated to POD range increase, the expected bias-like generated in Doppler can not be compensated by DD. FBE can cancel this bias.
 - If the FBE Modelling error are reduced (0.2 $mrad$ assumed), the SD2+FBE could result better than DD.
 - If some effect, associated to the fiducial stations, which have resulted very low in our assumptions (e.g Fiducial Multipath, fiducial Tropospheric and Fiducial Ionospheric) degrades from the considered values, the DD performances (and DD2+FBE) will also degrade.
- The most important error contributions are the short-term unstability of the clocks (GRAS and GPS), and the receiver thermal noise. In case of SD2+FBE, the clock frequency drift error has relevance.

Fig.4 shows the performance in bending angle under atmospheric diffraction conditions. It can be concluded that the back-propagation algorithm is able to recover the shape of the perturbation. A maximum refractivity gradient of $\partial N / \partial h|_{\max} = 57$ N - units/km , and a perturbation width of about 150 m has been considered. The reference bending angle for the comparison is computed with the inverse of the Abel Transform, from the refractivity profile.

Table 8. Percentage of data inside $\max(1mrad, 0.4\% \cdot a_{Neutral})$. Dense-wet atmosphere

Processing scheme	Slow Occultation	Normal Occultation
SD2+FBE	91.70	95.62
DD	97.71	100.00
DD2+FBE	97.40	100.00
ND+PBCC	96.70	100.00

Table 9: L1 & L2 & LC Average Bending angle error at 30 km (in $mrad$) in Slow velocity occultation taking average of different simulations. DD2+FBE, SD2+FBE, DD comparison

Error:	$a_{LC}^{30km} \text{ SD2+FBE}$	$a_{LC}^{30km} \text{ DD}$	$a_{LC}^{30km} \text{ DD2+FBE}$
Error free	0.0317	0.0308	0.0341
Relativistic Effects	0.0325	0.0310	0.0344
GRAS Hardware delays	0.0320	0.0356	0.0356
GRAS Thermal Noise	0.1538	0.1708	0.1248
GRAS AVAR	0.3521	0.0711	0.1463
GRAS freq offset	0.0452	0.0451	0.0483
GRAS freq drift	0.3921	0.0248	0.0147
GRAS multipath	0.2554	0.0930	0.2276
Metop Attitude	0.0771	0.0354	0.0667
POD bias	0.0316	0.0077	0.0331
POD harmonic	0.0325	0.0384	0.0358
GPS clock	0.2243	0.2573	0.2341
GPS SA	0.0212	0.0219	0.0156
Fiducial clock error	0.1485	0.0222	0.0790
Fiducial Thermal Noise	0.0671	0.0217	0.0770
Fiducial multipath	0.0314	0.0324	0.0282
Fiducial Tropospheric	0.0189	0.0189	0.0104
Fiducial Ionospheric	0.0249	0.0202	0.0228
FBE Modelling Error	0.2	0.0	0.2
All errors	0.5354	0.4098	0.3661
“all error + FBE modelling”	0.5715	0.4098	0.4172

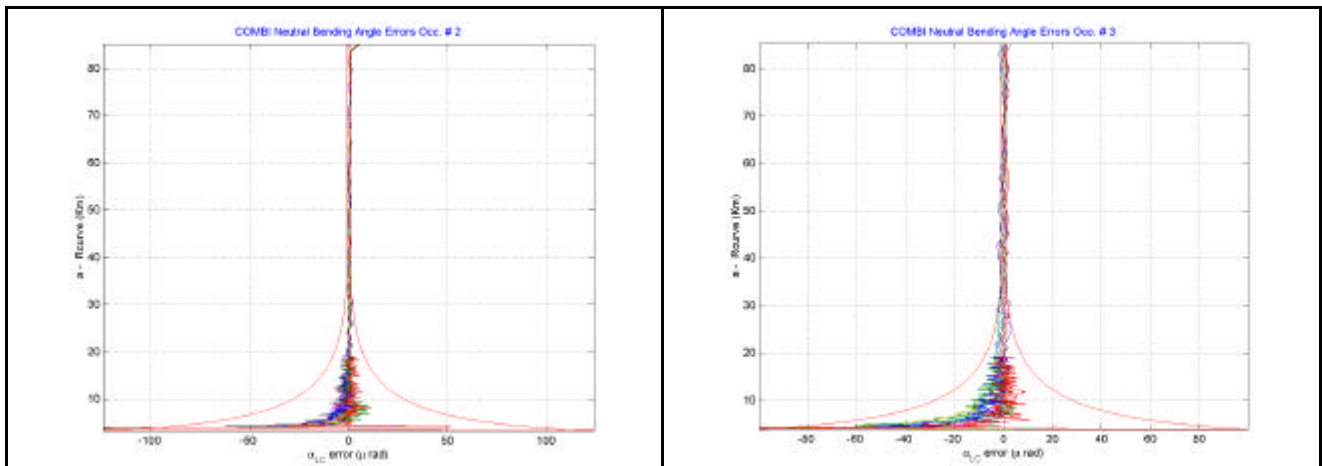


Fig. 3. Error in neutral bending angle with the SD2+FBE processing mode. Left plot is the normal velocity occultation and right plot is the slow velocity occultation.

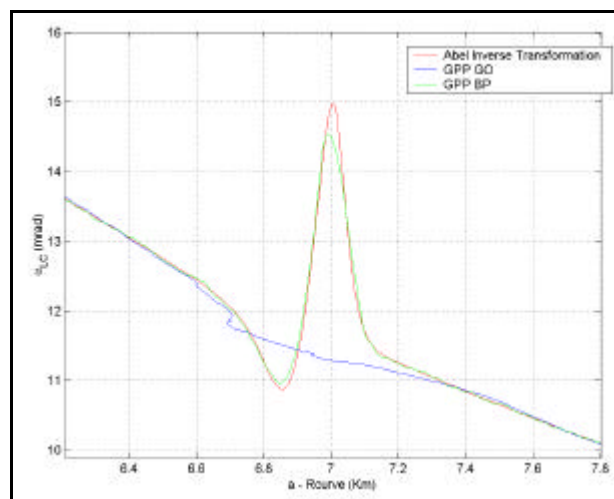


Fig. 4. Performances for retrieved neutral bending angle profile with respect to the reference simulated perturbation.

REFERENCES

- [1] C. Carrascosa-Sanz, A. J. Fernández, L. Tarabini, J. Christensen, M. Hägg, "Ground Processor Prototype for GPS Atmospheric Sounding". Proceedings of the GNSS 2001 International Conference, May 2001. Seville, Spain.
- [2] M. E. Gorbunov, A.S. Gurvich. "Microlab-1 Experiment: Multipath Effects in the Lower Troposphere", Journal of Geophysical Research, 103, 13819-13826, 1998
- [3] Kursinski et al: "Observing Earth's atmosphere with radio occultation measurements using the Global Positioning System". Journal of geophysical research, vol. 102, No. D19, pages 23429-23465, October 20, 1997
- [4] Meincke, M. D., Inversion Methods for Atmospheric Profiling with GPS Occultations, Ph. D. thesis, Scientific Report 99-11, Danish Meteorological Institute, 1999.
- [5] N. Ashby, J.J. Spilker Jr. "Introduction to Relativistic Effects on the Global Positioning System". Chapter 18 in Global Positioning System: Theory and Applications.
- [6] J. Christensen, J. Borman, C. Carrascosa-Sanz, M. Loiselet, "GRAS: GNSS Radio Occultation Receiver for Atmospheric Sounding". GNSS 2002 International Conference, May 2002. Copenhagen, Denmark.
- [7] M. Hägg, J. Christensen. "GRAS Ground Processor Prototype Specification". P-GRM-SPC-0017-SE v4 July 2003.
- [8] W. Lear, M. N. Montez, L. M. Rater, L.V. Zyla: "The effect of Selective Availability on orbit space vehicles equipped with SPS GPS receivers".
- [9] I Niell, A. E. "Global mapping functions for the atmosphere delay at radio wavelengths", J. Geophys. Res., 101, pp. 3227-3246, February 1996.
- [10] S. Bassiri and G. A. Hajj. "High order ionospheric effects on the global positioning system observables and means of modelling them". Manuscripta geodaeica (1993) 18: 280-289